

# Investigation of Water Management Dynamics on the Performance of a Ballard-Mark-V Proton Exchange Membrane Fuel Cell Stack System

Karthik Murugesan<sup>\*</sup>, Vijayachitra Senniappan

School of Electrical Sciences, Kongu Engineering College, Erode, Affiliated to Anna University, Chennai-600025, Tamil Nadu, India

\*E-mail: [karthik.prm@gmail.com](mailto:karthik.prm@gmail.com)

Received: 26 April 2013 / Accepted: 15 May 2013 / Published: 1 June 2013

---

Fuel cells are found to be the most promising source for the future era to meet out the energy demands. This is due to its green and clean energy production which increases the fuel cell research and development studies. This paper aims to bring out the importance of water management in a Proton Exchange Membrane Fuel Cell (PEMFC) stack system. At present several electrochemical models are available that predicts the steady state behavior for a specified set of operating conditions. However, such models have neglected the effect of water management dynamics on the polarization and performance characteristics. Hence a novel semi-empirical fuel cell dynamic model has been developed in a MATLAB/SIMULINK environment which predicts the complete transient and dynamic phenomena of the stack that incorporates the effect of membrane flooding and hydration/dehydration. The effect of water management dynamics over the system behavior is investigated and validated with the benchmark data obtained from a Ballard-Mark-V 5kW PEM fuel cell stack system. The results obtained show that the model responses fit well with the experimental results. Moreover, the model can predict the dynamic and transient response of stack voltage/power under a sudden change in load current. The developed model can be used to optimize the stack performance in terms of water management which facilitates in developing an optimized structural design of the fuel cell stack system for its scale-up.

---

**Keywords:** Ballard-Mark-V PEMFC stack, Membrane hydration, Membrane Water Content, humidification, Water flooding

## 1. INTRODUCTION

Over the past few years, Proton Exchange Membrane Fuel Cell (PEMFC) system has received much of great interest in research and development as it is one of the most promising alternative

sources of power for the future hybrid electric vehicle. Distributed Generation (DG) systems are the another broader area where PEM fuel cells can be employed irrespective of geographic location to yield an efficient performance when compared to solar (PV) and wind power generation. There are several classifications of fuel cells available in the market and they are classified based on the type of electrolyte material it utilizes [1]. Compared to other types of fuel cells, PEMFC has gained more of interest as they do not have moving parts, do not involve combustion, zero emission, high power density (power per cell active area), adaptable size, low operating temperature and are more reliable [2- 4].

However, PEM fuel cell technology is still obstructed in providing reliable power under dynamic load variations as they cannot react as quickly as desired to the load transients. This delay in response is not only because of time delay in initiating the electrochemical reaction and temperature dynamics inside the cell, but also due to mass transport delays imposed by the formation of liquid water on the cathode side of the fuel cell. Thus one of the major issues need to be studied and analyzed in developing a dynamic fuel cell model is to consider the mass transport limitation due to water dynamics [5-7] that may cause membrane hydration/dehydration or water flooding of electrolyte membrane used in the system.

Several works have been cited in the literature on steady state modeling [8-13] as well as dynamic modeling [3-4, 14- 21] of the fuel cell. Steady state modeling is developed only at cell level under preset standard operating circumstances. Barbir et al. [9, 10] have attempted to predict the performance of the fuel cell system for the standard operating temperatures, pressures and highlighted air supply interactions with the stack using the static polarization model developed by them. Mann et al. [8] have discussed the previously developed generic models for obtaining the steady state performance of the fuel cell system based on the operating variables such as pressure and temperature compositions and current density including membrane thickness and membrane ageing. Amphlett et al. [11, 12] have presented a parametric model for analyzing the steady state performance by combining the mechanistic and empirical modeling techniques with the use of empirical equations and the electrochemical reactions inside the fuel cell. Geyer et al. [13] proposed a simulation tool for analyzing the fuel cell system design using a thermodynamic potential equation based on partial pressures of reactants, current and cell temperature as input. In most of the above discussed models, modeling of fuel cell system is done based on the static polarization relations and empirical equations for a set of standard operating conditions.

Likewise, several dynamic models of the fuel cell system are available in the literature. All those models incorporate few levels of the dynamic variations such as temperature dynamics, hydrogen and air supply variations, humidity of the reactants etc. Wang et al [14] presented a dynamic model of the fuel cell system in which double-layer charging effect and temperature dynamics are taken into account. Result validation of this model is done based on the experimental results obtained from a 500 W Avista Labs SR-12 fuel stack system. Pathapati et al. [3] have developed a new dynamic model which incorporates double-layer charging effect, reactant flow dynamics, partial pressure variations and temperature dynamics. It predicts the transient dynamic response of cell voltage, stack temperature, flow rate and pressure variations under dynamic load variations and the results are validated with the benchmark results. Jung et al. [15] have proposed a computer dynamic model of

PEM fuel cell to study the voltage losses and temperature dynamics inside the stack. The model response is validated with the experimental results obtained from a Ballard-Nexa fuel cell system. Na et al. [16] have presented a dynamic nonlinear model for a PEMFC including gas inlet flow rates and pressure variations of the reactants as the control variables. The dynamic behavior of the stack modeled for the load variations are validated by the benchmark data obtained from literature. However, the model development is based on the assumptions of constant operating temperature of the stack with well humidified fuel flow reactants. Pukrushpan et al. [17] have developed a dynamic fuel cell model to capture the transient phenomena including the reactant flow behavior, partial pressure variations of the reactants as well as membrane humidity. Although this model can predict the behavior of the system that includes the membrane humidity modelling in its analysis, the obtained simulated results are not yet validated with any of the experimental results. Costa et al. [18] have formulated a dynamic model based on electrochemical equations and taken into consideration most of the chemical and physical characteristics of the cell. The validated results can able to predict only the internal losses and concentration effects behavior. Yalcinoz et al. [19] have presented a dynamic model for PEMFC including thermodynamic characteristics inside the stack relating water concentration and the resistance of the cell membrane. The model responses are compared against the simulation results obtained from the literature. Pasricha et al. [20] have developed a dynamic electric terminal model of a PEM Fuel cell including the temperature dependence of the stack and the model performance is validated using the experimental results collected from a SR-12 500W commercial PEM stack. Fuel cell model developed Lee et al. [21] consists of double layer charging effect, gas diffusion in the electrodes and thermodynamic characteristics that can be used for studying the electrical behavior of Ballard-Mark-V 5kW PEMFC stack system. The transient response of this model for a sudden change in load current is analyzed but the results are not validated with any experimental results. Although the dynamic model proposed by Jia et al. [4] is validated for a 20-cell stack fabricated by Singapore GasHub and FAC, it can describe the dynamic behavior of the stack having a well hydrated membrane that includes only the double layer charging effect in its study without considering the thermodynamic and water membrane hydration modeling.

The models of PEMFC reviewed here and those models that are not discussed here can be a good platform to understand the steady state and transient dynamic behavior of the system from different perspectives. But most of the models have not simultaneously incorporated the mass transport mechanism, temperature dynamics, partial pressure dynamics of the reactants, water dynamics in the form of membrane hydration/dehydration and double layer charging effect in their modeling. Further, the models discussed in the literature are neither validated with the experimental results though they include the water management dynamics nor they consider the water dynamics in its analysis with the proper validation of the simulation results for the other dynamics excluding the effect of water dynamics. Thus it is observed that none of the researchers have developed a dynamic model to investigate the dynamic behavior of the stack when unhumidified reactants are fed into it that relates the water dynamics. Hence an attempt is made in developing a model and it is presented in this paper that predicts the dynamic behavior of the stack accompanied with an unhydrated membrane.

The purpose of this paper is to develop a novel semi-empirical fuel cell dynamic model in a MATLAB/SIMULINK environment which is capable of predicting the complete transient dynamic phenomena of the stack that incorporates the effect of membrane flooding and hydration/dehydration in addition to other dynamics. Investigations are done on the PEMFC system behavior for the effect of water dynamics and are validated with the benchmark data published by Mann et al. [8] for the Ballard-Mark-V 5kW PEM fuel cell stack system. The comparison of the experimental results and simulation results show that the model can successfully forecast and estimate the characteristics of the fuel cell that facilitates the system analysis and its design optimization.

## 2. EXPERIMENTAL TEST SETUP OF BALLARD PEMFC

In this section, a description about the Ballard-Mark-V 5kW PEM fuel cell stack system is discussed. The description of the fuel cell system is firstly focussed on the theory of a single fuel cell structure governing the Ballard PEMFC test setup.

### 2.1 Theory of Fuel cell structure

PEMFC is a multi-input and multi-output, highly nonlinear and dynamically delayed system which involves mass flow transportation, electrochemical reaction, thermal conduction, water transportation. Hydrogen and oxygen are being used as a fuel at the anode and oxidant at the cathode respectively. These reactants are subjected to humidification before they reach the anode and cathode collector. Platinum is deposited as a layer on the surface of each electrode to speed up the electrochemical reaction. Also the cell consists of a Membrane Electrode Assembly (MEA), anode and cathode gas diffusion layers with two gas channels sandwiched between two coolant channels [23] as shown in Fig. 1. A schematic representation of a practical polymer electrolyte membrane fuel cell structure is given in Fig. 1.

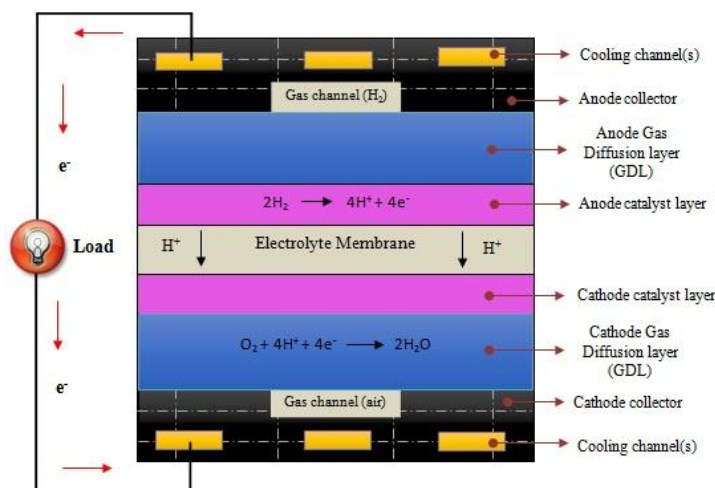


Figure 1. PEM Fuel cell structure overview.

The catalyst at the anode side causes the hydrogen atoms to discharge its electrons and become positively charged protons. The hydrogen ions diffuse from anode to cathode by migrating through the membrane assembly, while the electrons reach the cathode through an external electrical circuit doing useful work of providing electric power. These electrons along with the diffused hydrogen ions combine with oxygen from air to form water as a by-product which releases energy in the form of heat.



The theoretical open circuit potential of a single PEM fuel cell operating below 100°C is given by [24]:

$$E_o = \frac{-\Delta g}{nF} = 1.229 V \tag{4}$$

Here,  $n$  is the number of electrons involved in the electrochemical reaction,  $\Delta g$  is the change in Gibbs free energy and  $F$  is the Faradays constant. However, it is found that the working voltage is considerably less than the ideal open circuit voltage. This can be seen from the performance of a typical fuel cell in the form of polarization curve as depicted in Fig. 2. A graphical representation of a typical polarization curve that shows voltage losses in a PEM fuel against current density [15] is depicted in Fig. 2.

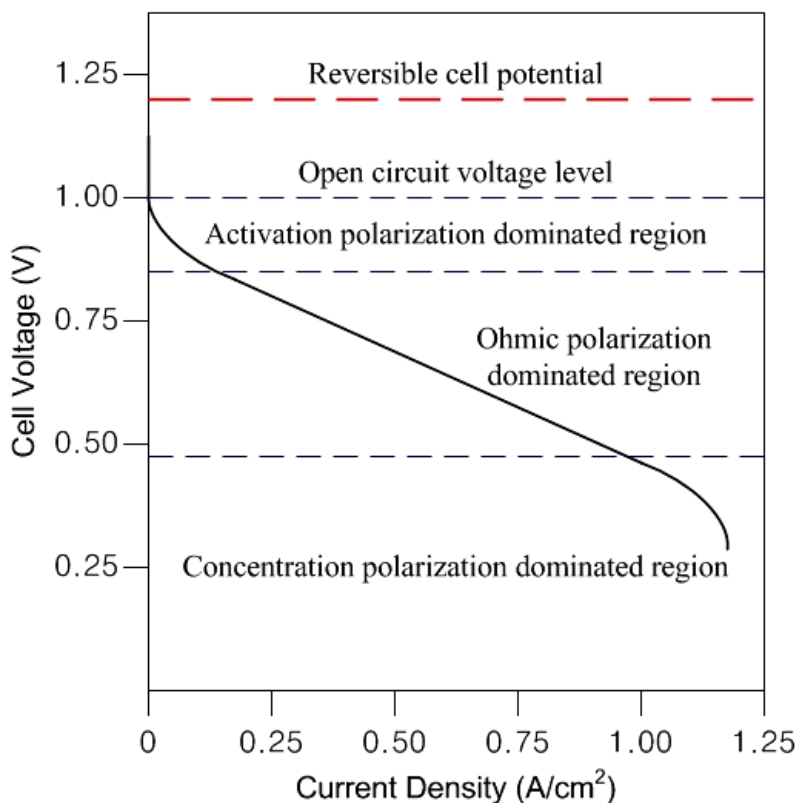


**Figure 2.** Typical Polarization curve of a PEM fuel cell voltage [15].

## 2.2 Description of the BALLARD PEMFC Test Setup

A simplified diagram of the Ballard-Mark-V 35-cell 5 kW PEMFC stack system taken for study is depicted in Fig. 3. The technical specifications of the Ballard-Mark-V PEM fuel cell system under study are discussed in this section.

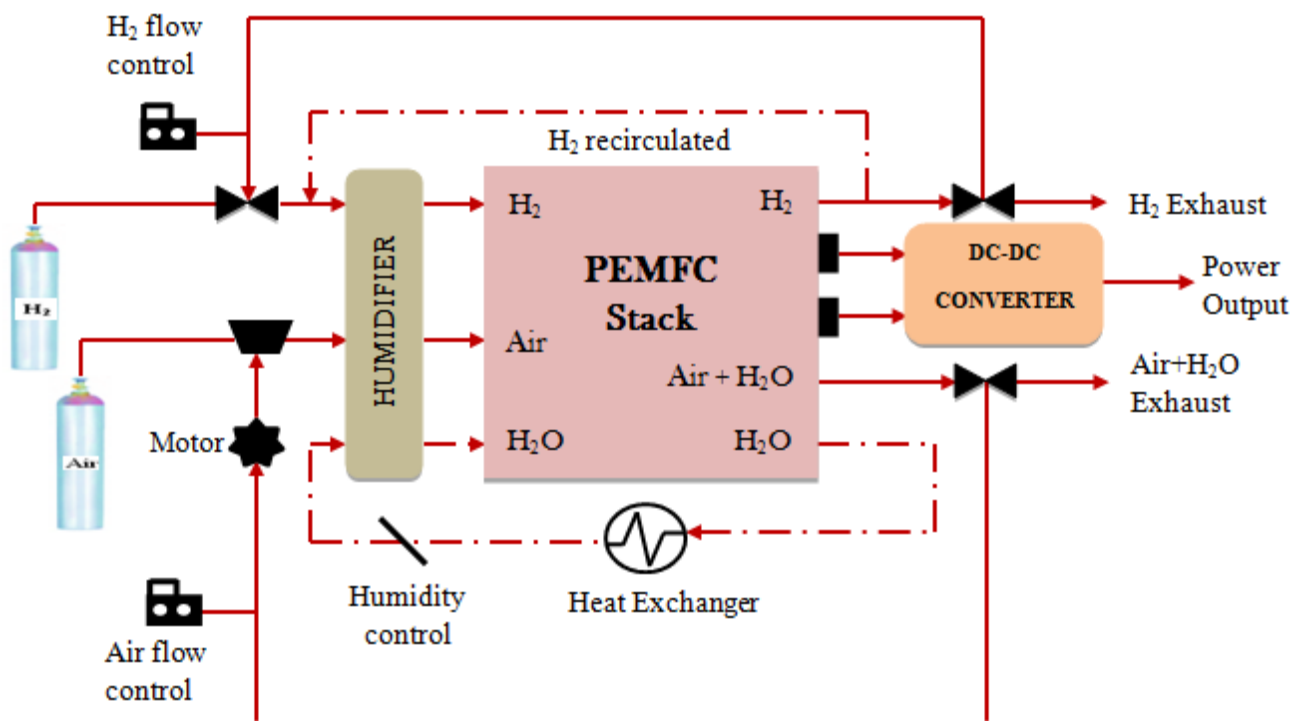


**Figure 3.** Simplified diagram of Ballard-Mark-V PEMFC stack system.

Ballard-Mark-V system manufactured by the Canadian company named Ballard [25] is used for investigating the water management dynamics in this paper. Ballard fuel cell stack system consists of 35 individual cells stacked in series. Each cell of the system basically consists of a Nafion 117 membrane and graphite electrodes embedded with a platinum catalyst in its Membrane Electrode Assembly with an active cell area of  $232 \text{ cm}^2$ . The stack measures approximately  $38 \text{ cm} \times 21 \text{ cm} \times 21 \text{ cm}$  and weighs approximately 43 kg [26]. The reactant gases such as pressurized hydrogen and air are supplied from external tanks and are humidified by means of a humidifier within the system. Pressurized and purified dry air is fed into the stack through humidifier from an air compressor. While the air pressure at the inlet and exhaust air at the outlet is kept at 3 bars by a back pressure regulator, the exhaust hydrogen at the outlet is re-circulated back at the anode with the hydrogen pressure at the inlet of the stack is maintained at 3 bars by a pressure regulator. Further, the operating temperature of the PEMFC stack is maintained at  $72^\circ\text{C}$  irrespective of change in temperature caused due to electrochemical reaction taking place inside the stack. Additional components such as heat exchanger, water management system and power conditioner are employed to achieve the optimal performance of the system.

### 3. MEMBRANE HYDRATION/FLOODING

Hydration of the Nafion 117 membrane is a very significant determinant for accomplishing the optimal performance and durability of a proton exchange membrane fuel cell system. Maintaining of sufficient membrane hydration is one of the important and critical issues of PEMFC operation. The necessity of maintaining the membrane with a proper hydration is to ensure the conduction of protons through it. If the membrane is not properly hydrated, it may either lead to drying of membrane or flooding of membrane. Dehydration occurs usually when pressurized hot gases are fed into the stack that adversely affects the lifetime of the membrane as it physically damages the membrane used. As a result, humidified reactants are fed into the stack. On the other hand, flooding of membrane occurs when the water removal rate is less than the water production rate at the cathodic chamber [7]. The flooding of membrane may also occur at lower current densities for the lower gas flow rates and stack temperature. This dehydration or flooding of membrane results in increase of polarization losses. For this, water management system is employed that monitors and manages the water removal rate from the stack.

Membrane dehydration or flooding of membrane is mainly because of water transport mechanism in the membrane that occurs inside the stack in three ways. Those contributing factors for the water transportation through the membrane is electro-osmotic drag from the anode to the cathode, back diffusion of water from cathode to anode and convective transfer because of pressure gradients inside the fuel cell stack. Thus apart from the humidification of the reactants to retain proper membrane hydration, Water management system is essential for the fuel stack system to prevent flooding of membrane. Considering all the aspects of membrane hydration, investigation of water management dynamics is found to be an essential critical design criterion to be considered and analyzed without neglecting it for predicting the cell performance characteristics.

### 4. MATHEMATICAL MODEL OF THE BALLARD PEMFC

In this section, a mathematical-nonlinear dynamic model is presented for illustrating the performance prediction of a PEM fuel cell stack. Investigation analysis of Water Management dynamics includes the following assumptions:

1. The model developed is one dimensional.
2. All gases are ideal and are distributed uniformly at a sufficiently constant rate.
3. Pure hydrogen gas is fed to the anode from a hydrogen fuel tank.
4. Liquid water is the only reaction product that always forms the stack.
5. The stack is equipped with a water management system to adjust the humidity level and water removal rate inside the system
6. Temperature at the cathode and anode are assumed to be constant throughout the operation and is assumed to be equal to the stack temperature.
7. Individual cells are lumped together to form a well designed stack with similar performance.

A fuel cell stack voltage model used in the present study estimates the stack voltage as a function of water management dynamics and is briefly discussed as follows:

#### 4.1 Electro dynamic potential of the cell

Considering the thermal behavior, mass transportation and the behavior due to water management dynamics, the basic output voltage produced by a single fuel cell is given by [14]

$$V_{cell} = E_{Nernst} - V_{act} - V_{ohm} - V_{conc} \tag{5}$$

The cell voltage drop is due to activation over potential  $V_{act}$  occurs at lower current density region, ohmic voltage drop  $V_{ohm}$  and concentration voltage drop  $V_{conc}$  at higher current density region.

The Nernst voltage equation used for describing the reversible potential of the cell is [21]

$$E_{Nernst} = E_o - 0.85 * 10^{-3} (T_{sfc} - 298.15) + 4.31 * 10^{-5} * T_{sfc} \left[ \ln(p_{H_2}) + \frac{1}{2} \ln(p_{O_2}) \right] \tag{6}$$

Stack temperature  $T_{sfc}$  of the fuel cell system, Partial pressure of hydrogen  $p_{H_2}$  and oxygen  $p_{O_2}$  inside the anode and cathode channel are the deciding dynamics of the reversible potential.

#### 4.2 Model of the Polarization losses

The activation over potential taking place on the surface of the electrodes is due to the limited rate of charge transfer [3]. Such activation polarization loss is expressed as [11]

$$V_{act} = (\xi_1 + \xi_2 T_{sfc} + \xi_3 T_{sfc} [\ln(C_{O_2})]) + \xi_4 T_{sfc} \ln(I_{sfc}) \tag{7}$$

where, the constant parametric coefficients  $\xi_n$  are obtained from the benchmark experimental data [8] published by Mann et al.  $I_{sfc}$  is the stack current of the fuel cell system expressed in Amperes.  $C_{O_2}$  is relatively depends on  $p_{O_2}$  and  $T_{sfc}$  that corresponds to the concentration of dissolved oxygen at the liquid interface.

$$C_{O_2} = \frac{p_{O_2}}{5.08 * 10^6 * \exp\left(\frac{4998}{T_{sfc}}\right)} \tag{8}$$

The ohmic polarization occurs as a result of electrolyte resistance, contact resistance at collector plates and graphite electrodes [4]. This ohmic polarization loss is linear since it is constant once when the cell is fabricated and this loss increases with increase in load. This can be expressed as

$$V_{ohm} = i * R_{ohm} \tag{9}$$

where,  $R_{ohm}$  is the internal electrical resistance that depends on the thickness of the membrane  $t_m$  and membrane conductivity  $\sigma_m$  which can be shown as [17]

$$R_{ohm} = \frac{t_m}{\sigma_m} \tag{10}$$

The membrane conductivity is determined by the following relation:

$$\sigma_m = b_1 \exp\left(b_2 \left(\frac{1}{303} - \frac{1}{T_{sfc}}\right)\right) \tag{11}$$

where,  $b_1$  is a function of membrane water content  $\lambda_m$  that varies when the water formation across the system varies.

$$b_1 = (b_{11} \lambda_m - b_{12}) \tag{12}$$



Here,  $b_2$ ,  $b_{11}$  and  $b_{12}$  are constants and is determined for Nafion 117 membrane whose values get varied depending on the type of membrane used.

In most of the model, the effect of concentration losses are neglected as it is not desirable to operate the cell in this region where the losses are high. But in this model, the concentration polarization loss is considered that occurs due to changes in the concentration of the reactants at higher current density region. The effect of concentration voltage drop is modeled by,

$$V_{con} = -B \ln \left( 1 - \frac{i}{i_{max}} \right) \tag{13}$$

where,  $i$  represents the actual current density of the cell (milli Amps/cm<sup>2</sup>) and  $i_{max}$  is kept constant usually in the range from 500 to 1500 milli Amps/cm<sup>2</sup>.  $B$  is a parametric coefficient that depends on the cell and its operation state.

Further, the double layer charging effect is another major factor that affects the activation polarization loss. This is because of the formation of charge near the electrode-membrane interface and behaves like a super capacitor. The equation that describes the effect is [3]

$$\frac{dV_{act}}{dt} = \frac{I}{C_{dl}} - \frac{V_{act}}{R_{act} * C_{dl}} \tag{14}$$

The charge double layer capacitance  $C_{dl}$  is usually in the order of few Farads and  $R_{act}$  can be determined by using  $V_{act}$  and  $I_{sfc}$  as per ohm's law.

### 4.3 Water dynamics

Water management system manages the humidity and the moisture in the system, keeping the fuel cell membrane saturated and simultaneously prevents the water from being accumulated at the cathode [27].

The Electrolyte membrane must be properly hydrated, requiring water to be evaporated at precisely the same rate that it is generated [28]. If water is evaporated too quickly, the membrane dries out and the resistance across it increases that leads to crack. Hence, hydrogen and oxygen combines directly and generates heat that will damage the fuel cell. On the other hand, if the water evaporation becomes too slow, then both the electrodes and membrane will flood. This also prevents the reactants from reaching the catalyst and stopping the reaction.

Thus calculating the water content  $\lambda_m$  in the membrane and membrane water flow across the membrane is essential for the water management system to maintain the proper hydration [22].

The total mass flow rate across the membrane  $f_{v,membr}$  is calculated by using vapour molar mass  $M_v$ , fuel cell active area  $A_{sfc}$  and number of cells used to form the stack.

$$f_{v,membr} = W_{v,membr} * M_v * A_{sfc} * n \tag{15}$$

where, the flow of water across the membrane is calculated by,

$$W_{v,membr} = w_d * \frac{i}{F} - D_w * \frac{(C_{v,ca} - C_{v,an})}{t_m} \tag{16}$$

The electro-osmotic drag coefficient  $w_d$  and water diffusion coefficient  $D_w$  are calculated from the water content in the membrane [5]:

$$w_d = 0.0029\lambda_m^2 + 0.05\lambda_m - 3.4 \times 10^{-19} \tag{17}$$

$$D_w = D_\lambda * \exp \left( 2416 \left( \frac{1}{303} - \frac{1}{T_{sfc}} \right) \right) \tag{18}$$

where,

$$D_\lambda = \begin{cases} 10^{-6} & , \lambda_m < 2 \\ 10^{-6} (1 + 2(\lambda_m - 2)) & , 2 \leq \lambda_m \leq 3 \\ 10^{-6} (3 - 1.67(\lambda_m - 3)) & , 3 \leq \lambda_m \leq 4.5 \\ 1.25 \times 10^{-6} & , \lambda_m \geq 4.5 \end{cases} \tag{19}$$

The water content in the membrane is calculated from the water activity  $a_i$

$$\lambda_i = \begin{cases} 0.043 + 17.81a_i - 39.85a_i^2 + 39.85 a_i^3 & , 0 \leq a_i \leq 1 \\ 14 + 1.4(a_i - 1) & , 1 \leq a_i \leq 3 \end{cases} \tag{20}$$

where,

$$a_m = \frac{a_{an} + a_{ca}}{2} \tag{21}$$

$T_{sfc}$  is the fuel cell temperature in Kelvin. The concentration of water at the anode and cathode side is a function of membrane water content.

$$C_{v,an} = \frac{\rho_{m,dry}}{\mathcal{M}_{m,dry}} \lambda_{an} \tag{22}$$

$$C_{v,ca} = \frac{\rho_{m,dry}}{\mathcal{M}_{m,dry}} \lambda_{ca} \tag{23}$$

where,  $\rho_{m,dry}$  (kg/m<sup>3</sup>) is the membrane dry density and  $\mathcal{M}_{m,dry}$  (kg/mol) is the membrane dry equivalent weight. The above equations used for the model development is based on the experimental results [6] published by Springer et al.

### 5. RESULTS AND DISCUSSION

In this section, a semi-empirical mathematical model for Ballard-Mark-V 5kW PEM fuel cell stack system developed is tested using MATLAB/SIMULINK environment. The specifications used for developing the Ballard model are given in Table 1. The empirical parameters used in this model development are listed in Table 2.

**Table 1.** Specifications of Ballard-Mark-V PEMFC system [16, 21]

Component	Value
Stack temperature	72° C
Active area of the cell	232 cm <sup>2</sup>
Anode Pressure	3 atm
Cathode Pressure	3 atm
Number of cells in the stack	35
Anode volume	0.005 m <sup>3</sup>
Cathode volume	0.01 m <sup>3</sup>
Membrane dry density	0.002 kg/cm <sup>3</sup>
Membrane dry Eq. weight	1.1 kg/mol
Membrane thickness	0.0178 cm

**Table 2.** Empirical parameters of Ballard-Mark-V system [6, 8, 25]

Parameter	Value
$\xi_1$	-0.948
$\xi_2$	0.00354
$\xi_3$	$7.6 \cdot 10^{-5}$
$\xi_4$	$-1.93 \cdot 10^{-4}$
$B$	0.016 V
$C_{dl}$	0.035 x232 F
$i_{max}$	1.5 A/cm <sup>2</sup>
$b_2$	1268
$b_{11}$	0.005139
$b_{12}$	0.00326

Simulation results are analyzed for the standard operating conditions and are validated with the experimental results as published by Mann et al. [8]. The results obtained for the model developed fit well with the steady state behavior of the Ballard-Mark-V system and thus can be used for predicting the dynamic and transient response under various degrees of membrane hydration level.

### 5.1 Experimental Setup

To validate the developed model in MATLAB /SIMULINK environment, the experimental results obtained from the test setup based on the Ballard 5kW PEM fuel cell is used [8]. The stack used in that study consists of 35-cells with a cross sectional area of 232 cm<sup>2</sup> for each cell. The membrane electrode assembly used in the model consists of Nafion 117 membrane. Humidified hydrogen and air are supplied at the anode and cathode respectively in which the hydrogen gas is recirculated at the anode. The performances of the Ballard stack model such as cell voltage and stack power versus current density characteristics are shown in Figs. 4 and 5.

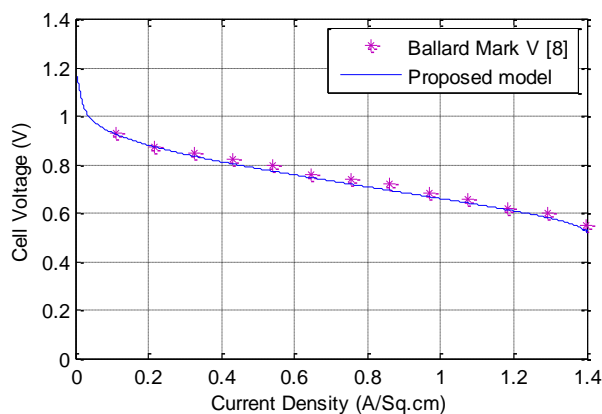


**Figure 4.** Model validation of the Ballard-Mark-V Polarization characteristics with the developed model for a single cell

### 5.2 Steady state behavior

The steady state characteristic in the form of polarization curve obtained by simulating the model for the standard operating conditions is validated with the experimental results [8] and is shown in Fig. 4. The steady state behavior of a single cell for the proposed model is obtained by simulating it with the standard operating temperature of 72 degree Celsius. The polarization curve is obtained by increasing the load current from 0A (no load current) to 325A over a period of 93 seconds. The predicted polarization curve of the semi-empirical model developed for the PEMFC has good agreement with the published experimental data as shown in Fig. 4. The model developed can perfectly predict the performance of the cell over a reasonably large range of voltages corresponding to current densities of as high as 1.4 A/cm<sup>2</sup>. The sudden drop in voltage at the start is due to activation loss and at the end of the curve is due to concentration loss. The linear drop in voltage in the middle between the activation and concentration losses is due to ohmic voltage losses that occur inside the stack.

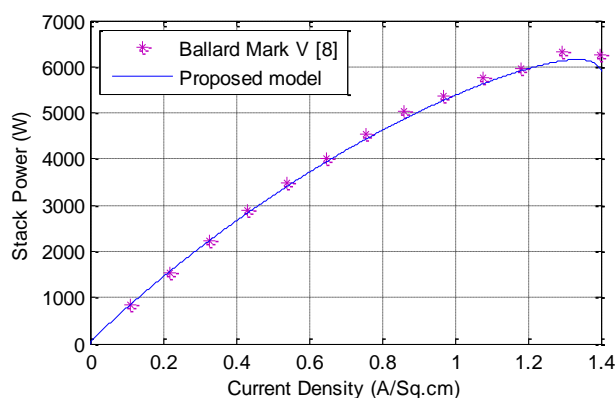


**Figure 5.** Stack Power – Current Density characteristics of Ballard-Mark-V PEMFC stack System operated at  $T_{stack}=72^{\circ}C$

Power versus current density characteristic of the PEM fuel cell stack obtained for the model developed and Ballard model is shown in Fig. 5. The experimental data of stack power is formulated using the polarization data [8] and current density. In this case also, the predicted power characteristic fits well with the experimental data. It can be seen from the power characteristics that the Fuel cell stack has delivered a maximum of 6.3 kW at about 1.29 A/cm<sup>2</sup>. The maximum power occurs very close to the concentration loss region and it starts to decrease when the load current is increased further in the concentration zone. This decrease in power output of the stack is due to the sharp drop in the stack voltage as it enters from ohmic region to concentration region. This necessitates the operation of the fuel cell in the ohmic region.

### 5.3 Effect of Membrane hydration

The effect of water hydration over the membrane has a significant impact on the cell performance [6] and is discussed in this section. Water management system includes humidifier that

serves in humidifying the feed gases into the stack assisting the membrane with proper water hydration. In addition to humidification, water management system serves in maintaining the proper hydration in the membrane by efficiently removing the water production rate at the cathode chamber [7]. Firstly, the profile of membrane water content  $\lambda_m$  for a membrane with proper hydration and without maintaining the water hydration level is analyzed and is shown in Fig. 6. Secondly, the effect of membrane hydration on the polarization loss is analyzed and depicted in Fig. 7. Thirdly, the effect of various degrees of water flooding over the cell performance is summarized and presented in Fig. 8. Lastly, the profile of power density curves for various degrees of water flooding is discussed and is shown in Fig. 9.

### 5.3.1 Effect on membrane water content

It can be seen that in Fig. 6, the membrane water content  $\lambda_m$  is maintained at 14 for different current densities that corresponds to a well hydrated [6] and humidified membrane. A well hydrated membrane is ensured by properly humidifying the fuel and the air before it enters into the stack [3, 24]. Hence the hydrogen fuel and the air are passed through the humidifier before it is fed into the anode/cathode chambers of the PEM fuel cell stack. In addition, the electrolyte membrane used has to be prevented from accumulation of water on it. This happens when the water removal rate is lesser than the water production rate at the cathode which leads to back diffusion of water [7] and results in flooding of membrane. As a result, water removal has to be efficiently done by the water management system and also by well maintained operating temperature of the stack.

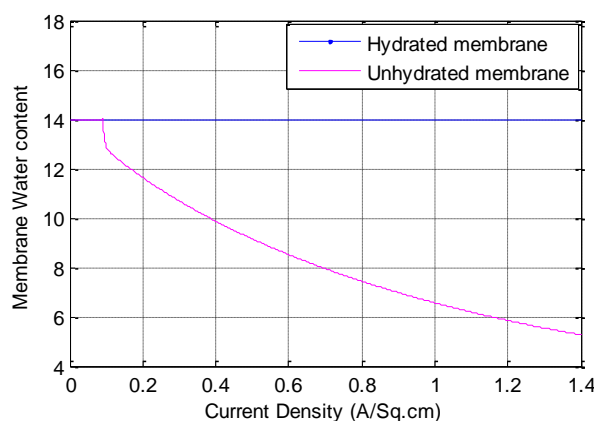


**Figure 6.** Membrane Water content for a hydrated and unhydrated membrane.

The profile shown in Fig. 6 also includes the membrane water content  $\lambda_m$  of a membrane used in the fuel cell stack when the reactants are not humidified. This corresponds to an unhydrated membrane when unhumidified fuel and air are passed on to the anode/cathode chamber of the PEM fuel cell stack and when the water removal rate equals the water production rate at the cathode. Initially at start up, the membrane water content  $\lambda_m$  is maintained at 14. Thus the stack performance is analyzed by using a membrane with nominal water content on it at the time of start up and the stack is

then gradually loaded in the absence of humidification system with proper water removal rate by the water management system. This leads to a decrease in the level of membrane water content towards 5 from 14 that correspond to a drying membrane when the current density reaches  $1.4 \text{ A/cm}^2$ . This drying membrane is due to hot pressurized hydrogen fuel and air passed on to the stack without humidification.

### 5.3.2 Effect on polarization losses

The effect of membrane water content over the cell voltage drop caused by ohmic loss that occurs inside the cell membrane is depicted in Fig. 7.

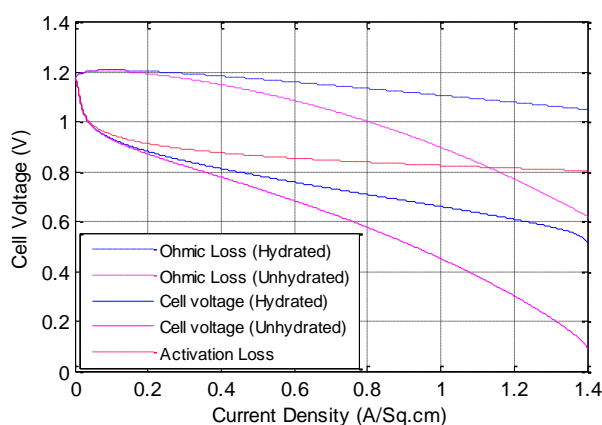


**Figure 7.** Voltage drop caused by ohmic loss due to hydrated and unhydrated membrane.

The effect of concentration loss over the cell voltage drop is neglected in this analysis as the optimal operating point lies only in the ohmic region [4]. Also, the membrane water content has no effect over the activation loss that occurs inside the cell and this can be seen from the cell voltage profile shown in Fig. 7. However, it is seen that the membrane water content has a significant impact over the ohmic loss under hydrated and unhydrated condition. The drop in cell voltage due to ohmic loss for a well hydrated membrane lies within 0.2 voltage while for an unhydrated membrane it drops about 0.6 volt as seen in Fig. 7. Also, the cell voltage comparison shown for a hydrated and unhydrated membrane clearly depicts the requirement of proper water hydration for the membrane to be used in the PEMFC stack so that the net cell voltage will be appreciable.

### 5.3.3 Effect of water flooding on polarization curve

In this section, cell voltage performance is analyzed for water flooding at various degrees of membrane water content  $\lambda_m$ . Effect of Membrane/water flooding over the polarization curve of a single cell used in Ballard-Mark-V fuel cell stack system is shown in Fig. 8. It illustrates the polarization curves for various degrees of membrane flooding with dissimilar membrane water content such as 14, 11, 7 and 5 that corresponds to the membrane without flooding, light, moderate and heavy

flooding respectively. It can be seen in the polarization profile that the slopes of the curves are heavily affected by the flooding of membrane. Accumulation of water occurs at cathode when the water removal rate is lesser than the water production rate which leads to water flooding of membrane [7]. This flooding of membrane is because of back diffusion of water accumulated at cathode towards anode [24]. The flooding of membrane prevents the membrane water content to be at 14.

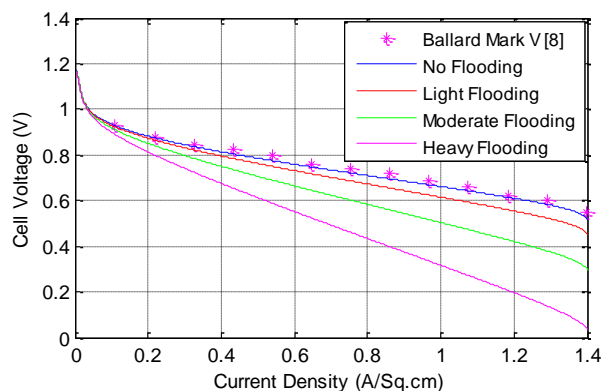


**Figure 8.** Polarization curves of a single cell for the effect of Membrane/water flooding.

Instead, the membrane water content will tend to decrease though the reactants are well humidified. This leads to a steeper decrease in the cell voltage at higher current densities where water production rate is higher particularly at moderate and heavy flooding. This necessitates the importance of proper functioning of water management system in the PEMFC stack that provides an appreciable performance.

#### 5.3.4 Effect of water flooding on power density

The power density versus current density curves of the PEMFC stack obtained from the experimental results of Ballard-Mark-V and the model proposed is depicted in Fig. 9 for the effects of different water flooding conditions. The model response fits well with the experimental data for the model developed that corresponds to the membrane without flooding condition. Though the operating point for the Ballard-Mark-V fuel cell system is 5kW for a power density of  $21.55 \text{ W/cm}^2$ , none of the authors has predicted the power performance of the stack beyond its operating point by maintaining MEA water balance. Hence an attempt is made in the proposed work for operating the stack beyond 5kW. It can be seen that the peak power density ( $27.18 \text{ W/cm}^2$ ) occurs near the fuel cell current density of  $1.29 \text{ A/cm}^2$  that corresponds to the rated current nearly of 300 A for the Ballard-Mark-V stack system under membrane without flooding condition. Beyond which the power density curve tends to decrease as the stack enters into the concentration zone.

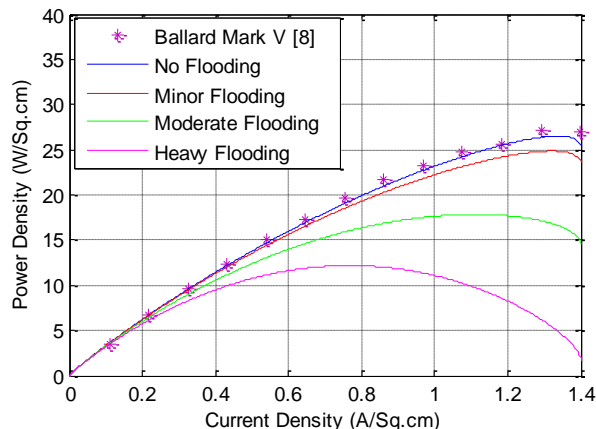


**Figure 9.** Stack Power Density curves of Ballard-Mark-V for different flooding conditions.

Also, Fig. 9 depicts the power density curves for various degrees of water flooding conditions. The power density curves show that the membrane assembly started to flood as the water removal rate is lesser than the water production rate at the cathode. It is noted that the significance of minor flooding over the power response is quite less when compared to the membrane without flooding condition. This is due to the fact that the membrane assembly still holds the conductive property of protons under minor flooding conditions. But during moderate and heavy flooding conditions, the occurrence of peak power density tends to decrease and particularly it is very less for the membrane assembly when subjected to heavy flooding. This is because the stack enters into the concentration zone much faster as the tendency of the membrane assembly fails to permit the flow of protons through it [7]. Hence to obtain the optimal performance of the PEMFC stack, water management system accompanied with it must maintain the proper hydration by efficiently removing the water production rate at the cathode chamber.

*5.4 Effect of water flooding at constant loading*

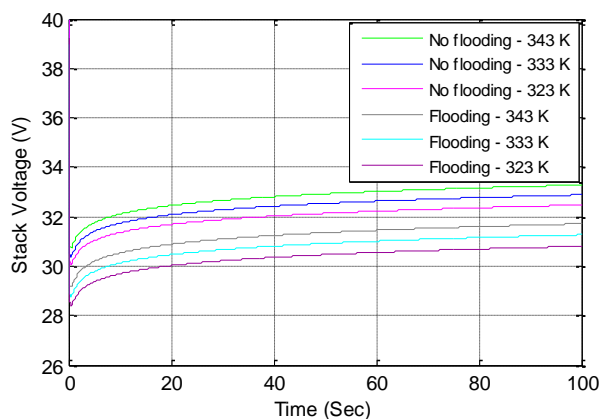


**Figure 10.** Stack voltage response at light loading current of 30A.



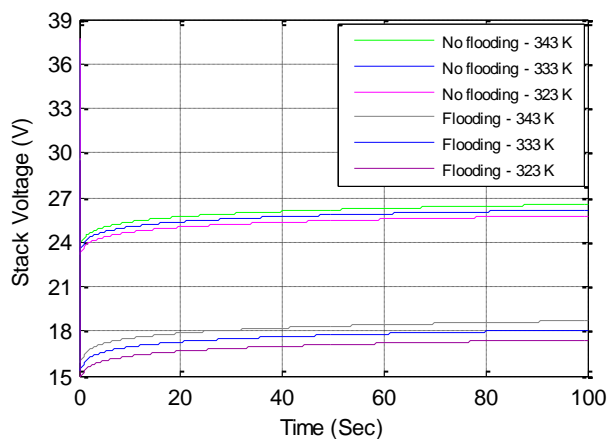


**Figure 11.** Stack voltage response at high Loading current of 150A.

Figs. 10 and 11 show the stack voltage response of the Ballard-Mark-V system when operated at different stack temperatures for a light loading current of 30A and high loading current of 150A respectively. It can be seen that the stack voltage is adversely affected by decreasing from its standard operating temperature of 70 degree Celsius to 60 and then to 50 degree Celsius. As discussed in section 5.3.4, the effect of flooding at light loading current of 30A is comparatively very less than that of flooding at high loading current of 150A. As depicted in Fig. 10, for a light loading at 30A, the effect of heavy flooding over the stack voltage is very less such that the drop in voltage between the operation under Flooding and No Flooding condition lies within 2 Volts. But for a high loading current of 150A, the effect of heavy flooding over the stack voltage is very high such that the drop in voltage between the operation under Flooding and No Flooding condition lies greater than 5 Volts. This necessitates the operation of the Ballard-Mark-V Fuel cell system with proper water management system that removes the water formation more effectively when operated at constant loading applications.

### 5.5 Dynamic behavior

To study the dynamic behavior of the developed model, changing step current is applied to the stack model for simulating the change in load and the corresponding characteristics are observed. The dynamic characteristic of the Ballard-Mark-V fuel cell stack includes the transient response of current on the stack voltage and power as a step load. Dynamic simulation of the developed model is done using the parameters listed in Table I and Table II and the simulation results are shown in Figs. 12, 13 and 14. It shows the dynamic response of stack voltage and power for the Ballard-Mark-V PEMFC stack system when the load changes between 90 A and 40A.

The dynamic property of the stack mainly depends on double layer charging effect, delay in reactant flow and temperature dynamics inside the stack [14]. In addition to the above said dynamic property that influences the stack performance, membrane water content plays a major role in contributing the transient response of the stack.

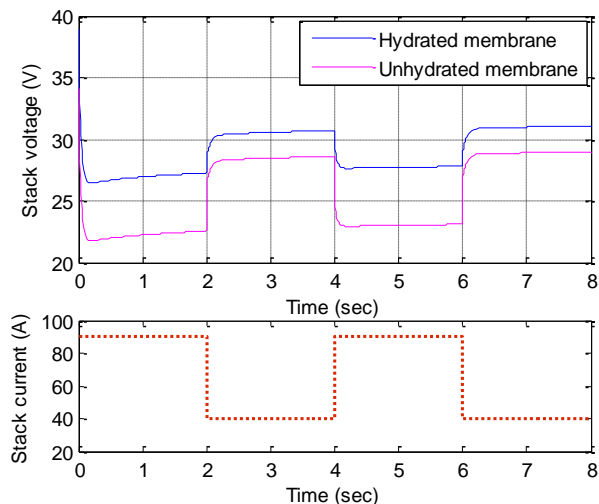


**Figure 12.** Dynamic response of stack output voltage when the load changes between 90 A and 40A.

The dynamic response of stack output voltage for the Ballard-Mark-V PEM fuel cell system is shown in Fig. 12 when the load current changes between 90A and 40A for a well hydrated and unhydrated membrane. Firstly, the dynamic response of stack output voltage is reviewed for the stack accompanied by a water management system that maintains the proper humidification of the reactants with an efficient water removal process. The output voltage changes from 27.34 to 28.55 V as the stack current stepped down from 90A to 40A at  $t = 2$  sec. This eventually decreases the voltage drop due to ohmic loss in the stack and reaches 30.56 V at 3 sec that almost maintained constant upto  $t = 4$  sec for about 30.72 V. When the current stepped up to 90 A from 40A at  $t = 4$  sec, the stack voltage decreases from 30.72 to 29.51 V. This ultimately increases the voltage drop due to ohmic loss in the stack and hence the stack voltage reaches to 27.72 V at 5 sec that almost remained constant till  $t = 6$  sec for about 27.84 V. This continues till the end of the simulation. Secondly, the dynamic response of stack output voltage is analyzed for the stack accompanied with a water management system that performs only the efficient water removal process and the reactants are unhumidified. The output voltage is 28.41 V at  $t = 3$  sec when the load current is 40A, whereas output voltage is 23.02 V at  $t = 5$  sec when the load current is 90A. This cycle is repeated till the end of the simulation.

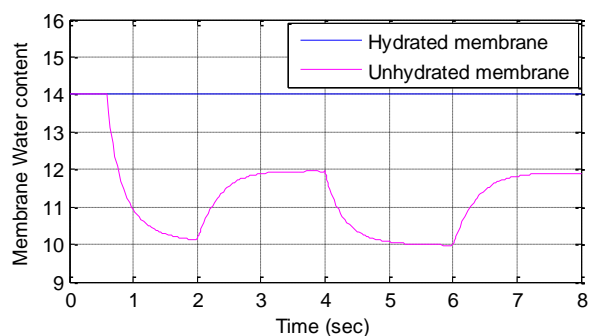


**Figure 13.** Membrane water content for a dynamic loading between 40 and 90A

It is inferred that operating the stack with unhumidified reactants causes a voltage drop of about 2.15 V and 4.7 V (approximately of about 5V) when the load current is 40A and 90A respectively. This drop in voltage of 2.15V at 40A is mainly due to the increase in membrane water content towards the nominal value of 14 since the membrane water content reaches near 12 for a low operating current of 40A as seen in Fig. 13. Similarly, the drop in voltage of 4.7V at 90A is mainly due to the decrease in membrane water content from the nominal value of 14 since the membrane water content reaches near 10 for a high operating current of 90A. The small delay in reaching near the stable value of 12 and 10 by the membrane water content at 40A and 90A is mainly due to the delay in decreased/increased feed reactant variations into the anode and cathode chamber from the respective gas tanks.

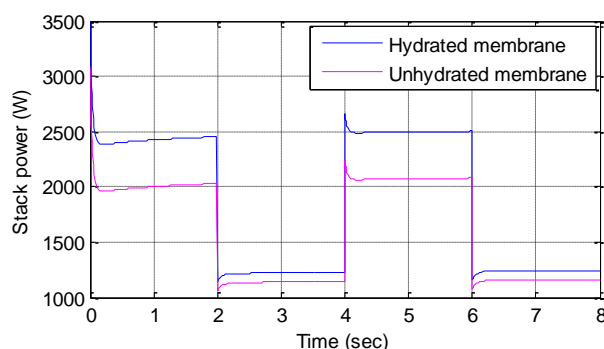


**Figure 14.** Dynamic response of stack output power when the load changes between 90A and 40A.

Dynamic stack output power for the model with a hydrated membrane has a peak value of 1.22kW at  $t = 3$  sec when the load current is 40A, whereas it is 2.49 kW at  $t = 5$  sec when the load current is 90A. The simulation is then continued for the model with unhydrated membrane. Stack output power for the model with unhydrated membrane has a peak value of 1.13kW at  $t = 3$  sec when the load current is 40A, while it is 2.07kW at  $t = 5$  sec when the load current is 90A. Thus there is a power loss of about 90 W at 40A and a power loss of about 420 W at 90A when the stack is operated with unhumidified reactants. Hence, a significant amount of power loss can be reduced if the stack has been equipped with a proper water management system that feeds well humidified reactants into it.

## 6. CONCLUSION

In this paper, a semi-empirical mathematical model is proposed for investigating the water management dynamics that predicts the transient and dynamic phenomena of a Ballard-Mark-V Proton Exchange Membrane Fuel Cell Stack System. Water management dynamics and double layer charging effect are taken into account in the model developed. The proposed model has been implemented in MATLAB/SIMULINK environment and the simulation analysis is carried out with a series of changing load, constant load and changing step load. The simulation results of the proposed dynamic model is tested and validated with the previously published experimental data of Ballard-Mark-V 5kW

system. Comparison of the results show that the proposed model yields surprising results which is viable, operable and valid as it can predict the steady state as well as transient electrical response of the PEMFC stack. Hence the developed model benefits in modeling and optimizing the structural design of the Fuel cell stack. Further, the model developed shows its potential in scaling up of the PEMFC stack in terms of water management.

## References

1. A.J. Appleby, F.R. Foulkes, *Fuel Cell Hand Book*, Seventh Ed., EG&G Technical Services, Inc.U.S.Department of Energy, United States (2004).
2. M.T. Gencoglu and Z. Ural, *Int. J. Hydrogen Energy.*, 34 (2009) 5242-5248.
3. P.R Pathapati, X. Xue, J. TangJ, *Int. J. Renew. Energy.*, 30 (2005) 1-22.
4. J. Jia, Q. Li, Y. Wang, Y.T. Cham and M. Han, *IEEE T Energy Conver.*, 24 (2009) 283-291.
5. T.V. Nguyen,R.E. White, *J. Electrochem. Soc.*, 140 (1993) 2178-2186.
6. T.E. Springer, T.A. Zawodzinski and S. Gottesfeld, *J. Electrochem. Soc.*, 138 (1991) 2334-2341.
7. H. Li and J.Z. et al., *J. Power Sources.*, 178 (2008) 103-117.
8. R.F. Mann, J.C.Amphlett, A.I. Michael and Hooper et al., *J. Power Sources.*, 80 (2000) 173–180.
9. F. Barbir, B. Balasubramanian and J. Neutzler, *Proceedings of the ASME Advanced Energy Systems*, 39 (1999) 305–315.
10. F. Barbir F, M. Fuchs, A. Husar and J. Neutzler, *Proceedings of SAE 2000 World Congress*, (2000) 63–70.
11. J.C. Amphlett, R.M. Baumert, R.F. Mann, B.A. Peppley and P.R. Roberge, *J. Electrochem. Soc.*, 142 (1995) 1–8.
12. J.C. Amphlett, R.M. Baumert, R.F. Mann, B.A. Peppley and P.R. Roberge, *J. Electrochem. Soc.*, 142 (1995) 9–15.
13. H.K. Geyer and R.K. Ahluwalia, GC Tool for fuel cell system design and analysis: user documentation, Argonne National Labs. ANL-98/9 (1998).
14. C. Wang, M. Hashem Nehrir and Steven.R. Shaw, *IEEE T Energy Conver.*, 20 (2005) 442-451.
15. Jee-Hoon Jung and Shehab Ahmed, *J. Power Electronics.*, 10 (2010) 739-748.
16. Woon Ki Na and Bei Gou, *IEEE T Energy Conver.*, 23 (2008) 179-190.
17. Jay.T. Pukrushpan, H. Peng and Anna.G. Stefanopoulou, *Proceedings of ASME International Mechanical Engineering Congress and Exposition*, (2002) 1-12.
18. R.A. Costa and J.R. Camacho, *J. Power Sources.*, 161 (2006) 1176-1182.
19. T. Yalcinoz and M.S. Alam, *J. Power Sources.*, 182 (2008) 168-174.
20. S. Pasricha and S.R. Shaw, *IEEE T Energy Conver.*, 21 (2006) 484-490.
21. Chien-hsing lee and Jian-TingYang, *J. Power Sources.*, 196 (2011) 3810-3823.
22. D. Ali and Daniel D. Aklil-D'Halluin, *Asia-Pacific Power and Energy Engineering Conference*, (2011) 1-5.
23. Y. Shan and Song-Yul Choe, *J. Power Sources.*, 145 (2005) 30-39.
24. James Larminie, Andrew Dicks, *Fuel Cell Systems Explained*, John Wiley & Sons Ltd, chichester (2003).
25. J.M. Correa, F.A. Farret and L.N. Canha, *Proceedings of 27<sup>th</sup> Annual Conference of the IEEE Industrial Electronics Society*, (2001) 141-146.
26. J.C. Amphlett, R.F. Mann, B.A. Peppley, P.R. Roberge and A. Rodrigues, *J. Power Sources.*, 61 (1996) 183-188.
27. J.T. Pukrushpan, A.G. Stefanpoulou and Huei peng, *IEEE Contr Syst Mag.*, (2004) 30-46.
28. J.T. Pukrushpan, A.G. Stefanpoulou and Huei peng, *J. Dyn Syst-T ASME.*, 126 (2004) 14-25.